

Precision Measurement of Drag Force Acting on a Spherical Body Dropping in the Air

Eko Satria^{1, a}, Mitra Djamal^{1, b}, Hendro^{1, c}, Akihiro Takita^{2, d}, Yusaku Fujii^{2, e}

¹High Theoretical Energy Physics and Instrumentation, Department of Physics, Bandung Institute of Technology, Bandung, INDONESIA

²Department of Electronic Engineering, Gunma University, 1-5-1 Tenjin-cho, Kiryu, Gunma, 376-0017, JAPAN

^aekosatria004@gmail.com, ^bmitra@fi.itb.ac.id, ^chendro@fi.itb.c.id, ^dtakita@gunma-u.ac.jp, ^efujii@gunma-u.ac.jp

Keywords: Air drag, Doppler shift frequency, drag force, optical interferometer

Abstract. This study proposes a method for measuring the drag force acting on a spherical body dropping in the air. A cube corner is attached to a spherical body. The velocity is accurately measured using an optical interferometer as the calculation of the Doppler shift frequency. The Doppler shift frequency is the difference between the beat frequency and rest frequency. The beat frequency is the frequency difference between the signal beam and the reference beam. The rest frequency is the difference of the two frequency of the laser. Then displacement, acceleration, force, mechanical energy, energy lost and the drag force acting on the spherical body can be calculated from information about velocity obtained.

1. Introduction

In fluid dynamics, drag force is the force that acts opposite to the relative motion of the objects in the fluid. This force exists between two moving liquid surfaces or fluids and solids in contact. Unlike other friction force, such as dry friction that does not depend on velocity, drag force depends on velocity. The drag force is proportional to velocity for laminar flow and proportional to the square of the velocity for turbulent flow. Measurement of air drag is needed in many areas such as aircraft [1], [2], sports equipment [3]–[5], and bridge construction [6], [7].

Measurement of the drag force is very complex. A direct measurement such as using the wind tunnel, although accurate, but highly impractical [8], for example, the wind tunnel testing facility is accessible and very expensive.

Due to the difficulty of the drag force measurement, a lot of researcher estimates the projected frontal area to estimate the air drag [9], [10]. Estimation of the projected frontal area assumes that the drag coefficient is constant. However, the drag coefficient is not constant. The drag coefficient depends on many parameters i.e. Reynolds number, shape, orientation, secondary motion, the density ratio of particle and fluid, the intensity of fluid turbulence and acceleration of particle/fluid [11]–[14].

Several methods have been carried out in the measurement of air drag, i.e. using the wind tunnel [1]–[4] and using a high speed camera [15]. But there are drawbacks of these methods. As described previously, the use of wind tunnel is impractical and expensive, then, the fixture needed to support the object to be tested in the wind tunnel will probably affect the measured drag [16]. Then, measurements with the use of camera cannot measure the whole movement due to limitations of the field of vision of the camera [16].

The authors have previously developed precision mechanical measurement methods known as the Levitation Mass Method. In this Levitation Mass Method (LMM), the inertial force of mass levitated using aerostatic linear bearing is used as the reference force imposed on the object to be tested. The inertial force is measured accurately using the optical interferometer. In this measurement method, this force is not measured directly. Force and other mechanical parameters such as

acceleration, velocity, and displacement derived from measurements of Doppler frequency shift using a laser interferometer [17]–[21]. LMM measurement method has been modified to measure the impact force of water surface and produced the accurate measurement of the impact force [22].

In this paper, we proposed the method for precision measurement of the drag force acting on a spherical body dropping in the air using modified LMM measurement. Measurement and data processing to obtain information about the drag force will be explained in this paper.

2. Experiment

Figure 1 shows the experimental set-up used in the precision measurement of the drag force acting on a spherical body falling in the air. This research used the spherical iron with the diameter 30.2 mm as shown in Figure 2. A cube corner prism with the diameter 12.7 mm was placed on the iron ball which will reflect the light from the optical laser interferometer to be able to find out information about the movement of the iron ball accurately. The total mass of the spherical body system is 93.88 grams. The detail of the spherical body system shown in Figure 3.

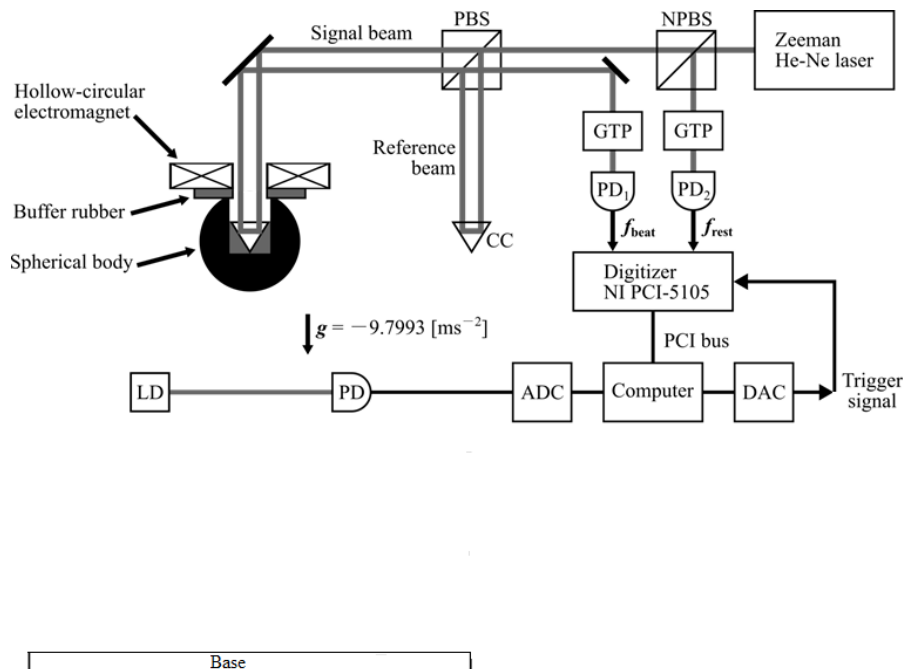


Fig. 1. Experimental setup. CC = cube-corner prism, PBS = polarizing beam splitter, NPBS = non-polarizing beam splitter, GTP = Glan-Thompson prism, PD = photodiode, LD = laser diode, ADC = analog-to-digital converter, DAC = digital-to-analog converter

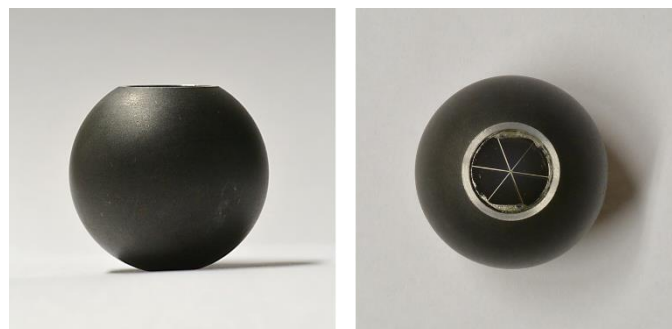


Fig. 2. Photographs of the spherical body

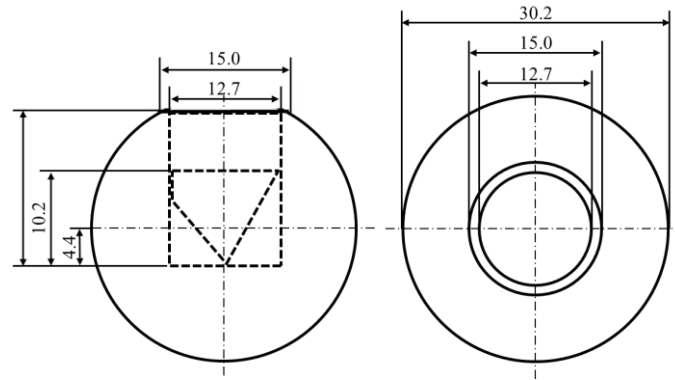


Fig. 3. Dimensions of the spherical body

The motion of the spherical body is affected by some forces, those forces are gravity, drag force and buoyancy force. The presence of the drag force and buoyancy force that act opposite to the direction of motion cause the loss of mechanical energy. By knowing the falling velocity and displacement, then the mechanical energy of the falling spherical body can be obtained. The velocity is obtained from the measured value of the Doppler frequency shift of the interferometer $f_{Doppler}$, which is expressed as follows:

$$v = \frac{\lambda_{air} \cdot f_{Doppler}}{2} \quad (1)$$

$$f_{Doppler} = -(f_{beat} - f_{rest}) \quad (2)$$

Where λ_{air} is the wavelength of the laser beam, f_{beat} is the beat frequency. The beat frequency is the frequency difference between the signal beam and the reference beam. f_{rest} is the frequency of rest, when the spherical body at rest on the stand, f_{beat} and f_{rest} will have the same value. Then, from this velocity information, the displacement of the spherical body can be calculated.

The sum of drag force and buoyancy force acting on the spherical body is obtained by calculating the mechanical energy lost at any time of the spherical body. The mechanical energy is the total energy which is the sum of kinetic energy and potential energy of the spherical body, where

$$E_k = \frac{m \cdot v^2}{2} \quad (3)$$

$$E_p = m \cdot g \cdot h \quad (4)$$

$$E_M = E_k + E_p \quad (5)$$

Then the sum of drag force and buoyancy force acting on the spherical body is calculated using the equation

$$D_i + F_B = \frac{E_{M(i+1)} - E_{M_i}}{h_{(i+1)} - h_i} \quad (6)$$

$$F_B = \rho_{air} \cdot g \cdot V_{spherical_body} \quad (7)$$

So, the drag force acting on the spherical object can be obtained by

$$D_i = \frac{E_{M(i+1)} - E_{M_i}}{h_{(i+1)} - h_i} - \rho_{air} \cdot g \cdot V_{spherical_body} \quad (8)$$

Where E_k is the kinetic energy, E_p is potential energy, E_M is mechanical energy, m is the mass of spherical body (93.88 grams), v is the velocity of spherical body, g is the gravitational acceleration, approximately 9.795 m/s^2 at the experimental room, h is the height (position) of the spherical body, F_B is the buoyancy force, ρ_{air} is the density of air (1.2047 kg/m^3), $V_{spherical_body}$ is the volume of the spherical body and D is the drag force acting on the spherical body.

An optical interferometer is used to measure the velocities accurately. A Zeeman-type two-wavelength He-Ne laser with two frequencies with orthogonal polarization is used as the light source. The difference of the two frequencies; i.e. the rest frequency f_{rest} , is Approximately 3.0 MHz.

A digitizer (NI PCI-5105, National Instruments Corp., USA) was used to record signals from the output of PD1 and PD2 with sample number 5 M for each channel, with the sampling rate 30 M samples per second and the resolution 8 bits. Measurement duration is 0.020 s. Frequency f_{beat} and f_{rest} accurately obtained from the digitized waveform output signal of PD1 and PD2 using Zero-Crossing Fitting Method (ZFM). In the calculation of the frequency by using ZFM, all zero crossing at each sampling interval is used to calculate the frequency. In this study, sampling interval used is $N = 1000$ periods.

In this experiment, a hollow circular electromagnet is used to hold and release the spherical body. This electromagnet can be switched on and off manually. Then the recording of data by the digitizer is initiated using the trigger signal generated by the digital-to-analog-converter (DAC). This signal is activated by a light switch which is a combination of a laser diode and photodiode.

3. Result

Figure 4 shows the data processing of precision measurement of the drag force acting on a spherical body dropping in the air. Velocity v , displacement h , mechanical energy E_m can be calculated from the information of f_{beat} and f_{rest} obtained from the optical interferometer.

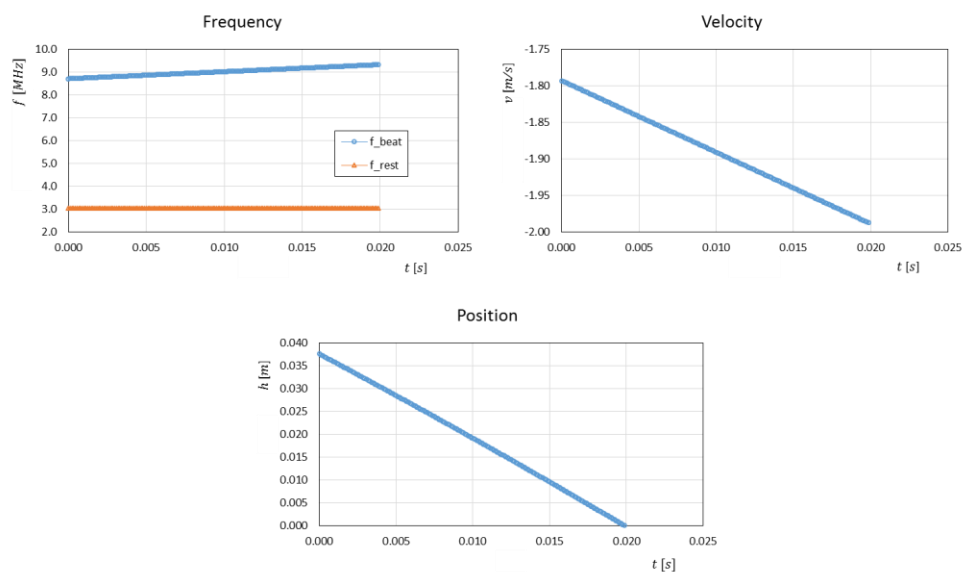


Fig. 4. Data processing procedure: Calculation of velocity and position from frequency

The presence of noise in the optical interferometer causes the decrease in the mechanical energy measured using this optical interferometer is not smooth. As seen in figure 5, fitting is done to the chart of mechanical energy decline of the spherical body. Fitting is done using order 2 polynomial fitting.

Then the result is used to calculate the energy lost from the spherical body, and the drag force acting on the spherical body can be obtained.

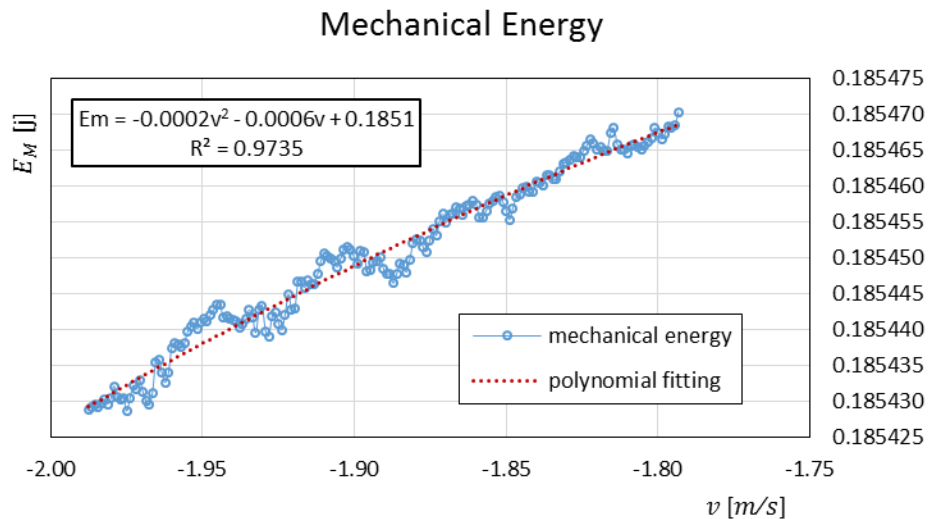


Fig. 5. Decrease in mechanical energy due to air drag

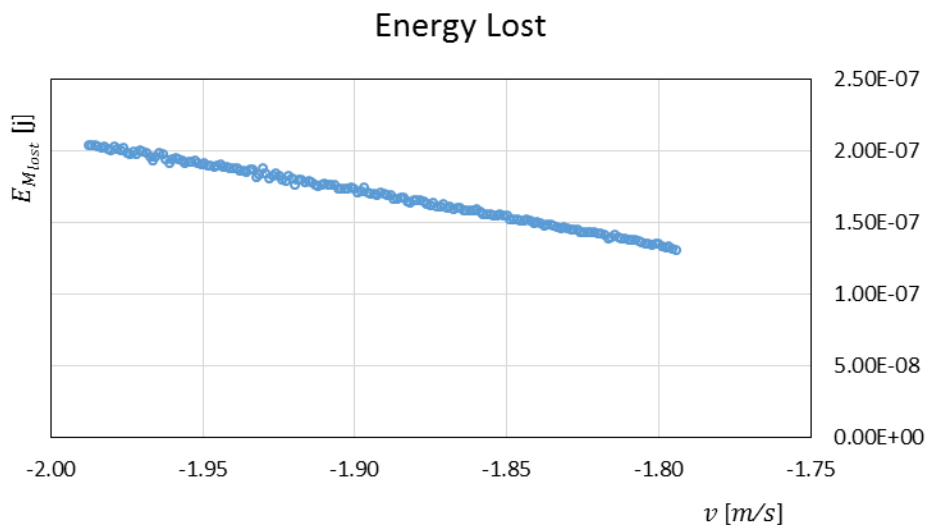


Fig. 6. Energy lost obtained from fitted mechanical energy decrease

From Figure 7, it appears that the drag force acting on the spherical body highly dependent on the velocity. It is observed that the greater the velocity of the falling spherical body, the greater is the drag force acting on it.

Theoretically, the resistance force acting on an object moving in the air is the result of the acceleration of the air that being pushed to pass up the object. The object will push the air with a volume equal to the multiplication of the projected area and velocity. Acceleration of the gas is proportional to the velocity of the object relative to the air. The drag force is defined as

$$D = \frac{1}{2} \cdot \rho \cdot v^2 \cdot C_D \cdot A \quad (9)$$

Where D is the drag force, ρ is the density of air, v is the relative velocity of the material to the air, A is the projected area (πr^2 for a sphere), and C_D is the drag coefficient of the object. For a sphere, C_D is defined by the following equation [23].

$$C_D = \frac{24}{Re} + \frac{2.6 \left(\frac{Re}{5.0} \right)}{1 + \left(\frac{Re}{5.0} \right)^{1.52}} + \frac{0.411 \left(\frac{Re}{2.63 \times 10^5} \right)^{-7.94}}{1 + \left(\frac{Re}{2.63 \times 10^5} \right)^{-8.00}} + \frac{0.25 \left(\frac{Re}{10^6} \right)}{1 + \left(\frac{Re}{10^6} \right)} \quad (10)$$

Re is the Reynold number, a dimensionless number which is the ratio of inertial force to the viscous force. Re is expressed by the following equation

$$Re = \frac{v \cdot d}{\nu} \quad (11)$$

Where d is the diameter of the sphere and ν is the kinematic viscosity of air.

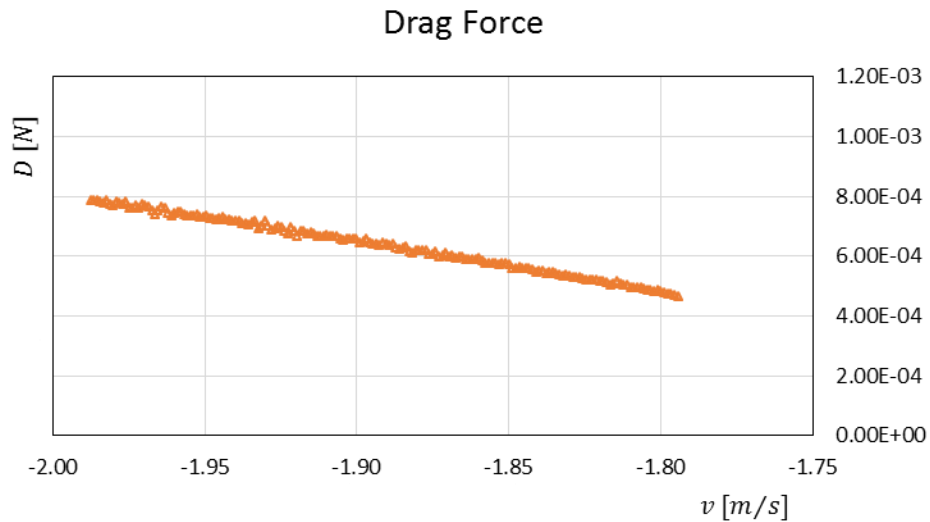


Fig. 7. Drag force obtained from energy lost

Figure 8 shows the comparison between the drag force obtained using the proposed method and the drag force obtained theoretically using equation 9. From the graph, it can be seen that the experimental value using the proposed method produces slightly different results with the values obtained by theoretical calculation. This is due to the uncertainty caused by several things described in the discussion. Correlation between the velocity of the spherical body and the drag force can be observed clearly.

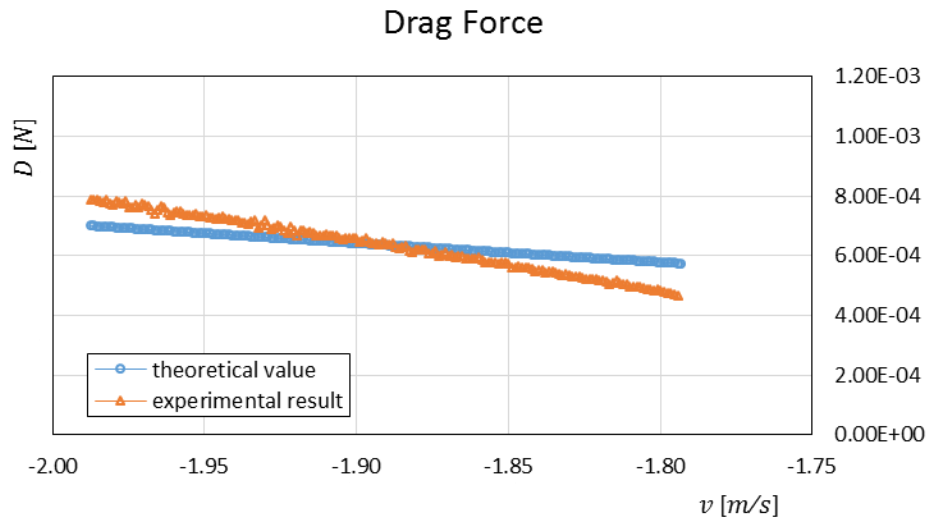


Fig. 8. Drag force obtained using proposed method and theoretical calculation.

4. Discussion

In this research there are some things that can cause uncertainty in the measurement of the drag force acting on a spherical body as it is falling in the air. These include:

a. Optical alignment

This uncertainty caused by the inclination of the signal beam by 1 mrad.

b. Mass calibration

Uncertainty in the measurement of the mass using the electric balance is 0.001 g. The uncertainty in the measurement due to the uncertainty of the mass will cause the uncertainty of the kinetic energy and potential energy that will cause the uncertainty of the drag obtained.

c. Acceleration due to gravity

Acceleration of gravity at the experimental room is estimated to be 9.795 m/s^2 . The uncertainty of gravity will lead to uncertainty in the calculation of potential energy and will contribute to the uncertainty in the calculation of the drag force.

d. Noise from optical interferometer

e. Frequency estimation using ZFM

Errors in estimates of frequency f_{beat} and f_{rest} will lead to errors in the calculation of velocity and position so that the errors will occur in the energy calculation. The errors obtained in the calculation of energy will result in error in the calculation of the drag force in the air.

5. Conclusion

A new method for the precision measurement of the drag force acting on a spherical body falling in the air is proposed. The velocity of the spherical body is measured accurately using the optical interferometer with the sampling interval 1 ms. A cube corner prism is placed in the spherical body, so that the velocity can be measured accurately using the optical interferometer. The measured velocity is then used to obtain the position, the energy lost and the drag force of the spherical body.

Acknowledgements

This research was supported in part by a research-aid fund of the Asahi Glass Foundation, a research-aid fund of the NSK Foundation for the Advancement of Mechatronics (NSK-FAM) and the grant-in-aid for Scientific Research (B) 24360156 (KAKENHI 24360156).

References

- [1] A. Koreanschi et al., "Optimization and design of a morphing wing tip aircraft demonstrator for drag reduction at low speeds, Part II – Experimental validation using infra-red transition measurements during wind tunnel tests," *Chin. J. Aeronaut.*
- [2] J. van der Vooren, "On drag and lift analysis of transport aircraft from wind tunnel measurements," *Aerosp. Sci. Technol.*, vol. 12, no. 4, pp. 337–345, Jun. 2008.
- [3] K. Okawa, Y. Komori, T. Miyazaki, S. Taguchi, and H. Sugiura, "Free Flight and Wind Tunnel Measurements of the Drag Exerted on an Archery Arrow," *Procedia Eng.*, vol. 60, pp. 67–72, 2013.
- [4] F. Alam, H. Chowdhury, S. George, I. Mustary, and G. Zimmer, "Aerodynamic Drag Measurements of FIFA-approved Footballs," *Procedia Eng.*, vol. 72, pp. 703–708, 2014.
- [5] J. R. Kensrud and L. V. Smith, "In situ drag measurements of sports balls," *ResearchGate*, vol. 2, no. 2, pp. 2437–2442, Jun. 2010.
- [6] A. Acampora, J. H. G. Macdonald, C. T. Georgakis, and N. Nikitas, "Identification of aeroelastic forces and static drag coefficients of a twin cable bridge stay from full-scale ambient vibration measurements," *J. Wind Eng. Ind. Aerodyn.*, vol. 124, pp. 90–98, Jan. 2014.
- [7] Y. Han, H. Chen, C. S. Cai, G. Xu, L. Shen, and P. Hu, "Numerical analysis on the difference of drag force coefficients of bridge deck sections between the global force and pressure distribution methods," *J. Wind Eng. Ind. Aerodyn.*, vol. 159, pp. 65–79, Dec. 2016.
- [8] J. E. Peterman, A. C. Lim, R. I. Ignatz, A. G. Edwards, and W. C. Byrnes, "Field-measured drag area is a key correlate of level cycling time trial performance," *PeerJ*, vol. 3, p. e1144, Aug. 2015.
- [9] D. Heil, "Body mass scaling of projected frontal area in competitive cyclists," *Eur. J. Appl. Physiol.*, vol. 85, no. 3–4, pp. 358–366, Aug. 2001.
- [10] T. OLDS and S. OLIVE, "Methodological considerations in the determination of projected frontal area in cyclists," *J. Sports Sci.*, vol. 17, no. 4, pp. 335–345, Jan. 1999.
- [11] A. Haider and O. Levenspiel, "Drag coefficient and terminal velocity of spherical and nonspherical particles," *Powder Technol.*, vol. 58, no. 1, pp. 63–70, May 1989.
- [12] R. P. Chhabra, L. Agarwal, and N. K. Sinha, "Drag on non-spherical particles: an evaluation of available methods," *Powder Technol.*, vol. 101, no. 3, pp. 288–295, Mar. 1999.
- [13] E. Loth, "Drag of non-spherical solid particles of regular and irregular shape," *Powder Technol.*, vol. 182, no. 3, pp. 342–353, Mar. 2008.
- [14] A. Hölzer and M. Sommerfeld, "New simple correlation formula for the drag coefficient of non-spherical particles," *Powder Technol.*, vol. 184, no. 3, pp. 361–365, Jun. 2008.
- [15] B. Krueger, S. Wirtz, and V. Scherer, "Measurement of drag coefficients of non-spherical particles with a camera-based method," *Powder Technol.*, vol. 278, pp. 157–170, Jul. 2015.

- [16] G. Bagheri and C. Bonadonna, "On the drag of freely falling non-spherical particles," *Powder Technol.*, vol. 301, pp. 526–544, Nov. 2016.
- [17] Y. Fujii, A. Takita, J. Kaewkhao, M. Djamal, and T. Yamaguchi, "Precision Force Measurement Using the Levitation Mass Method (LMM)," *Appl. Mech. Mater.*, vol. 103, pp. 1–8, 2012.
- [18] M. Djamal et al., "Dynamic Characteristics Measurements of a Force Transducer Against Small and Short-Duration Impact Forces," *Metrol. Meas. Syst.*, vol. 21, no. 1, Jan. 2014.
- [19] T. Jin et al., "High-speed impact test using an inertial mass and an optical interferometer," *Rev. Sci. Instrum.*, vol. 84, no. 7, p. 75116, Jul. 2013.
- [20] N. Miyashita, K. Watanabe, A. Takita, M. Djamal, T. Yamaguchi, and Y. Fujii, "Measurement of Dynamic Responses of a Force Sensor against Small Impact Forces with Various Durations," *Key Eng. Mater.*, vol. 698, pp. 73–79, 2016.
- [21] M. Djamal, I. A. Prayogi, K. Watanabe, A. Takita, and Y. Fujii, "New Method for Evaluating Dynamic Characteristics of Cantilever Spring of Vibration Sensor," *Adv. Mater. Res.*, vol. 1025–1026, pp. 372–378, 2014.
- [22] R. Araki et al., "Impact force measurement of a spherical body dropping onto a water surface," *Rev. Sci. Instrum.*, vol. 85, no. 7, 2014.
- [23] F. A. Morrison, *An Introduction to Fluid Mechanics. Cambridge University Press*, 2013.